

Conf-9305159--3

UCRL-JC-114922
PREPRINT

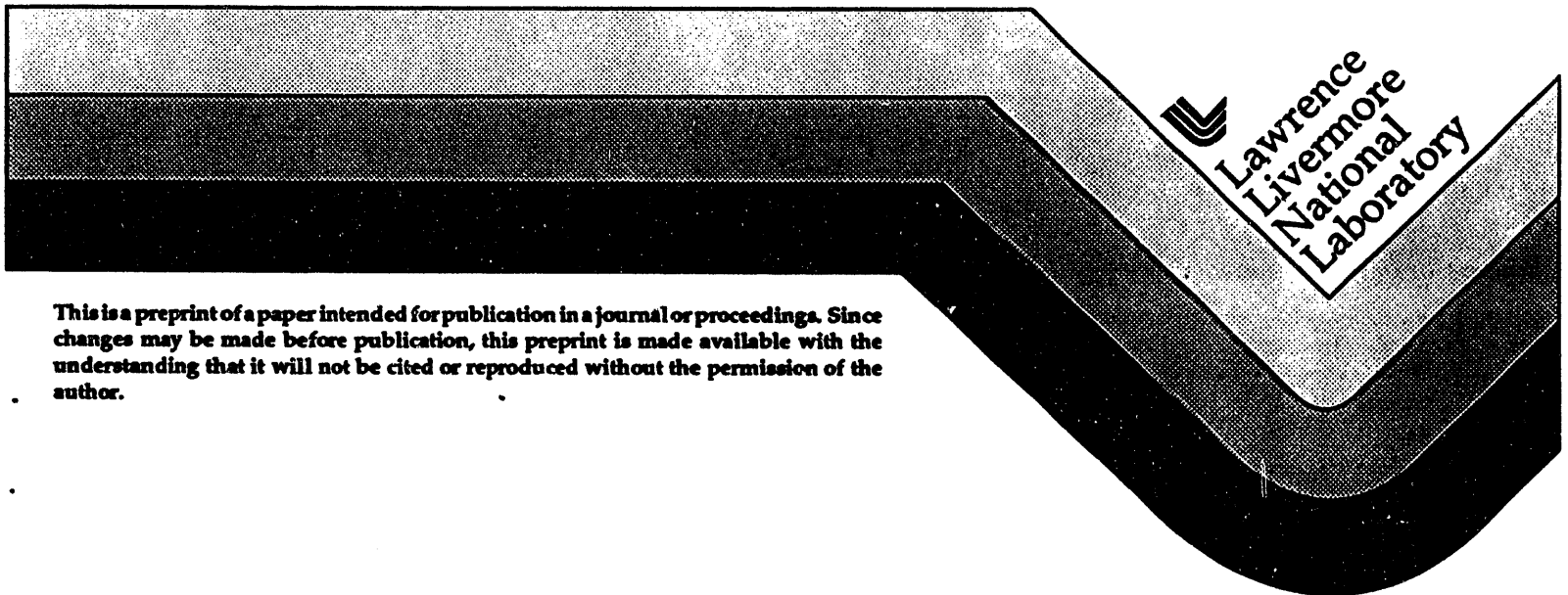
RECEIVED
AUG 09 1993
OSTI

X-ray Plasma Source Design Simulations

Charlie Cerjan
Lawrence Livermore National Laboratory

This paper was prepared for submittal to :
OSA Proceedings on Soft X-ray Projection Lithography '93
May 10-12, 1993, Monterey, CA

July 1993



This is a preprint of a paper intended for publication in a journal or proceedings. Since changes may be made before publication, this preprint is made available with the understanding that it will not be cited or reproduced without the permission of the author.

MASTER

DISTRIBUTION OF THIS DOCUMENT IS UNLIMITED

jc

DISCLAIMER

This document was prepared as an account of work sponsored by an agency of the United States Government. Neither the United States Government nor the University of California nor any of their employees, makes any warranty, express or implied, or assumes any legal liability or responsibility for the accuracy, completeness, or usefulness of any information, apparatus, product, or process disclosed, or represents that its use would not infringe privately owned rights. Reference herein to any specific commercial products, process, or service by trade name, trademark, manufacturer, or otherwise, does not necessarily constitute or imply its endorsement, recommendation, or favoring by the United States Government or the University of California. The views and opinions of authors expressed herein do not necessarily state or reflect those of the United States Government or the University of California, and shall not be used for advertising or product endorsement purposes.

X-ray Plasma Source Design Simulations

Charles Cerjan

POB 808 L-438

Lawrence Livermore National Laboratory

Livermore, CA 94550

Abstract

The optimization of soft x-ray production from a laser-produced plasma for lithographic applications is discussed in the context of recent experiments by R. Kauffman *et al.* which indicate that a conversion efficiency of 0.01 can be obtained with Sn targets at modest laser intensity. Computer simulations of the experiments delineate the critical phenomena underlying these high conversion efficiencies, especially the role of hydrodynamic expansion and radiative emission. Qualitative features of the experiments are reproduced including the transition from one-dimensional to two-dimensional flow. The quantitative discrepancy is ascribed to incorrect initiation of the ablating plasma and to inadequate atomic transition rate evaluation.

1. Introduction

Several different soft x-ray sources have been proposed for lithographic applications, especially laser-produced plasmas and radiation from synchrotron bending magnets. The development of each of these proposed sources is currently under active experimental investigation with the eventual goal of optimal performance. Although each source has its advantages, the research presented below will exclusively focus on the issues underlying the efficient production of soft x-rays in a narrow spectral band determined by constraints imposed by the Mo/Si multilayer mirrors. The recently proposed projection lithography scheme of Ceglio and Hawryluk [1] requires a conversion efficiency of about 0.01 into 2π steradians within a 2.2 eV band centered at 95 eV. This requirement is essentially determined by the maximal reflectance of these mirrors, while accounting for the overall system design constraints.

Although the specific application is dictated by this particular projection scheme, the general issues raised below will be germane to the design of most laser-produced plasma sources. In the low-intensity regimes considered here, there are two major concerns for maximization of the conversion efficiency: first, the energy balance between hydrodynamic losses and radiative output; second, the appropriate nuclear charge and ionization stage of the emitting material. Since bound-state to bound-state transitions are much more effective than free-bound processes for producing the narrow-band spectral output, the design of the laser-plasma source will depend critically on channeling the input laser energy into the production of the necessary electron temperature and density needed to maintain the appropriate ionization stages for the greatest length of time.

The first of these items – hydrodynamic expansion – determines the partition of input energy into convective losses and radiative emission. The primary issue is to minimize the energy losses incurred by expansion and subsequent cooling as the plasma evolves. The ablating plasma should remain as collimated as possible along the incoming laser axis. The controlling factors in the experimental design become the laser focal spot size, laser pulse length, the energy on target, and the laser light frequency. Clearly, for the same amount of

energy on target, an increasingly narrow focus will produce more radial divergence in the plasma. The other factors can be similarly manipulated to produce more or less expansion. In general, the laser intensity will be the important scaling quantity, so, for example, if the laser focus is doubled the energy should increase four-fold to maintain the same plasma conditions.

The second important design criterion is the choice of target material, which means the selection of the effective charge and electronic configuration of the emitting ionization stages. In other words, the radiative emission must be directed into the useful output band of interest. The plasma must achieve conditions such that it is out of equilibrium with electron collisional processes which in turn implies that the emission will significantly depart from black-body (Planckian) emission. Estimates of the radiation temperature required to produce the observed narrow-band conversion efficiencies are greater than the deposited laser energy. The observation of spectral lines [2] provides unambiguous evidence of departure from black-body conditions. Furthermore, the ionized material should have large dipole-allowed transitions in the required spectral band so that effective use can be made of the non-equilibrium conditions. For the plasma sources envisioned in these simulations, the non-equilibrium regime is reached in the ablation zone. The material is heated to the appropriate ionization stages and then expands before the excited electronic configurations can be quenched by electron collisions. In this sense, the so-called collisional-radiative treatment should apply: the non-equilibrium conditions are prepared by electron collisions but only relax by radiative processes [3].

The remainder of this paper is divided into two sections. In the following section, the details and results of various computer simulations are presented. The last section describes the comparison with some experimental data and offers some conclusions concerning the scope of the simulations.

2. Numerical Details and Results

The principal computational program used for the simulations is the three-temperature

(radiation, electron and ion) Lagrangean hydrodynamic code LASNEX [4]. This code has been extensively used in Inertial Confinement Fusion (ICF) applications and is capable of using various levels of sophistication in the treatment of the atomic rate processes, ranging from in-line average-atom descriptions to completely detailed rate information.

All the simulations were performed in two dimensions with cylindrical geometry since the relative contribution of hydrodynamic expansion to the energy balance is crucial. A non-local thermodynamic equilibrium (NLTE) treatment of the plasma was also found to be essential for the reasons delineated above. The choice of atomic rates included was dictated by the availability of the data for the ionization stages considered. In practice, this limitation forces the simulations to use a scaled-hydrogenic treatment of the energy levels and associated collisional and radiative rates. This approach is of course not capable of spectroscopic accuracy, but can be useful when examining more averaged quantities such as relatively broad-band conversion efficiency. Detailed, spectroscopically accurate, rates can be calculated with substantially more effort but this approach is not practical for wide-ranging parameter studies.

The simulations were chosen to mimic the experimental conditions [2]: 0.25 Joules of 0.532 μm light were deposited into a variable focal diameter with a Gaussian temporal pulse length of 7.5 nsec and a smooth “flat-top” spatial distribution. The experimental spatial and temporal profile was not used, though in principle these variations could also be included. The conversion efficiency into several spectral bands was monitored: the narrow band of interest at 95 eV; the broad-band Be-window band (72.5 eV to 110 eV); and the total spectral output.

The results of these simulations for the conversion efficiency of Sn within the narrow (2.2 eV) band are plotted in Figure 1 as a function of laser intensity. The trend with intensity is reproduced by the calculations but clearly the peak values are not. Since the precise determination of the output band is difficult for the scaled-hydrogenic rates used, a better gauge of the accuracy can be obtained by examining the total photon output. Such a

determination was made for Ta at several intensities, where, due to calibration errors, only the total output above 45 eV was measured. Comparable calculations to the observations are presented in Table 1. Again, the overall trend is approximately the same with the simulations remaining about 30% too low.

3. Discussion

The qualitative trend – the maximum in the conversion efficiency as a function of intensity – in the experimental and calculational results can be understood as the onset of two-dimensional expansion effects at constant focus and to over-ionization of the plasma leading to population of higher stages which emit at higher energies. Since the dominant effects occur in the coronal region, it might be expected that simple self-similar, scaling, relations are applicable to estimate two-dimensional cooling effects. Using the well-known relationship for the electron temperature (with units indicated in parentheses), $T_e(keV)$, as a function of intensity, $I(1 \times 10^{14} W/cm^2)$ [5],

$$T_e(keV) = 0.6(I\lambda^2/f)^{2/3}, \quad (3.1)$$

with flux-limiter, f , and wavelength, $\lambda(1.064 \mu m)$, the rate of expansion in the direction perpendicular to the laser can be estimated. That is, when the laser pulse length multiplied by the sound speed exceeds the focal diameter, then convective losses can be expected to contribute significantly. The sound speed, $c_s(cm/sec)$, is [5]

$$c_s = 3 \times 10^7 (ZT_e/A)^{1/2}, \quad (3.2)$$

where Z is the effective nuclear charge and A is the atomic weight. For a pulse length of 7.5 ns, the simultaneous solution of these relations yields a value of 140 μm for the focal diameter which corresponds to a laser intensity of 1.7×10^{11} in approximate agreement with the observations and the more detailed computer simulations.

This scaling relation also indicates the expected rise in electron temperature as the intensity increases. Once the electron temperature exceeds the optimal value for production

and maintenance of those ionization stages contributing to the narrow-band emission, the plasma becomes more efficient at higher energy emission, outside the desired range. The identification of the appropriate ionization stages for different materials is the subject of ongoing research and will be elucidated in future reports.

The quantitative discrepancy between the calculations and observations most likely arises from two principal causes: the atomic rates inaccurately describe the position and strength of the dominant radiative transitions and the initial hydrodynamic expansion of the cold material is inadequately described. Clearly, if there are dominant spectral features misplaced in energy then these transitions cannot contribute to the expected output since they were excluded. Likewise, even if the dominant transitions are included in the correct energy positions, any inaccuracy in their calculated strength will also adversely affect the predicted output. The only way to correct this failing is to perform more detailed atomic physics calculations.

The results of a more extensive calculation for Sn reveals that the dominant spectral feature observed at lower electron temperatures is a 6f-4d transition in the Sn^{+6} ionization stage. At higher temperatures, 4d-4p transitions in Sn^{+7} to Sn^{13} contribute. Large dipole-allowed transitions are predicted between 92 and 97 eV. Several other ionization neighboring ionization stages also contribute within a few eV of this value, so a more complete simulation must incorporate these contributions also, which adds substantially to the complexity of the problem. The evaluation of these additional contributions is in progress.

Another possible difficulty is the early-time heating and expansion of the cold material. It is likely that discrepancies in the total conversion efficiency between predictions and observations is due to thermodynamic inconsistencies in the simulation below 10 eV, since the initiation of the plasma is not usually well-described by an inverse Bremsstrahlung absorption mechanism. In the low-intensity regime considered here, the initial incorrect density gradients will persist for a substantial fraction of the laser pulse thereby skewing the eventual energy partition into hydrodynamic and radiative contributions. For the simulations in this

low intensity regime, the laser absorption and material expansion is over-estimated leading to lower conversion efficiencies than those observed. This inadequacy is quite difficult to correct, although a more thorough investigation of the initiation stage might suggest a simple correction. These issues are also being actively investigated.

Experimental issues should also be reassessed to ensure the validity of the reported values. It is important to recall that these experimental measurements were simple one-point measurements – a fixed angle of observation was used – and the results were assumed to have a Lambertian distribution. These items will be addressed in future experiments.

In conclusion, several of the salient issues important to x-ray plasma source design have been addressed. Predictive accuracy for the calculations is not yet available, but reasonable qualitative agreement exists for the cases studied. The simulations are thus a useful tool for material and laser parameter studies, and as an aid in the interpretation of experimental results.

Acknowledgements

The author is pleased to acknowledge useful and entertaining discussions with D. W. Phillion, R. Spitzer and R. L. Kauffman on many aspects of this research; R. London deserves credit for improvements in the manuscript. Work at the Lawrence Livermore National Laboratory is performed under the auspices of the U.S. Department of Energy, administered by the University of California under Contract No. W-7405-Eng-48.

References

- [1] N. M. Ceglio and A. M. Hawryluk, "Soft X-ray Projection Lithography Design," OSA Proceedings on Soft-x-ray Projection Lithography, v. 12, J. Bokor, ed., pp5-9, (Optical Society of America, Washington D. C., 1991).
- [2] R. L. Kauffman, D. W. Phillion, and R. Spitzer, "X-ray production at 130 A from laser-produced plasmas for x-ray projection lithography applications," (*Applied Optics*, this issue).
- [3] D. Colombant and G. F. Tonon, "X-ray emission in laser-produced plasmas," *J. Appl. Phys.*, **44**, 3524(1973).
- [4] G. B. Zimmerman and W. L. Kruer, "Numerical Simulation of Laser Initiated Fusion," *Comm. Plasma Phys. Cont. Thermonuclear Fusion*, **2**, 85(1975).
- [5] C. Max, "Physics of the Coronal Plasma," in Les Houches, Session XXXIV, 1980 - Interaction Laser-Plasma/Laser-Plasma Interaction, R. Balian and J. C. Adam, eds., pp302-410, (North-Holland, Amsterdam, 1982).

Table 1

Total conversion efficiency experiment and theory comparison
for Ta as a function of laser intensity
(numbers in parentheses indicate powers of 10)

I_{exp}	η_{exp}	I_{th}	η_{th}
5.23(9)	0.16	5.00(9)	0.12
1.01(10)	0.33	1.00(10)	0.20
2.68(11)	0.59	1.00(11)	0.44
1.42(13)	0.66	1.00(13)	0.54

Figure Captions

Figure 1: Sn narrow-band conversion efficiency plotted as a function of intensity.

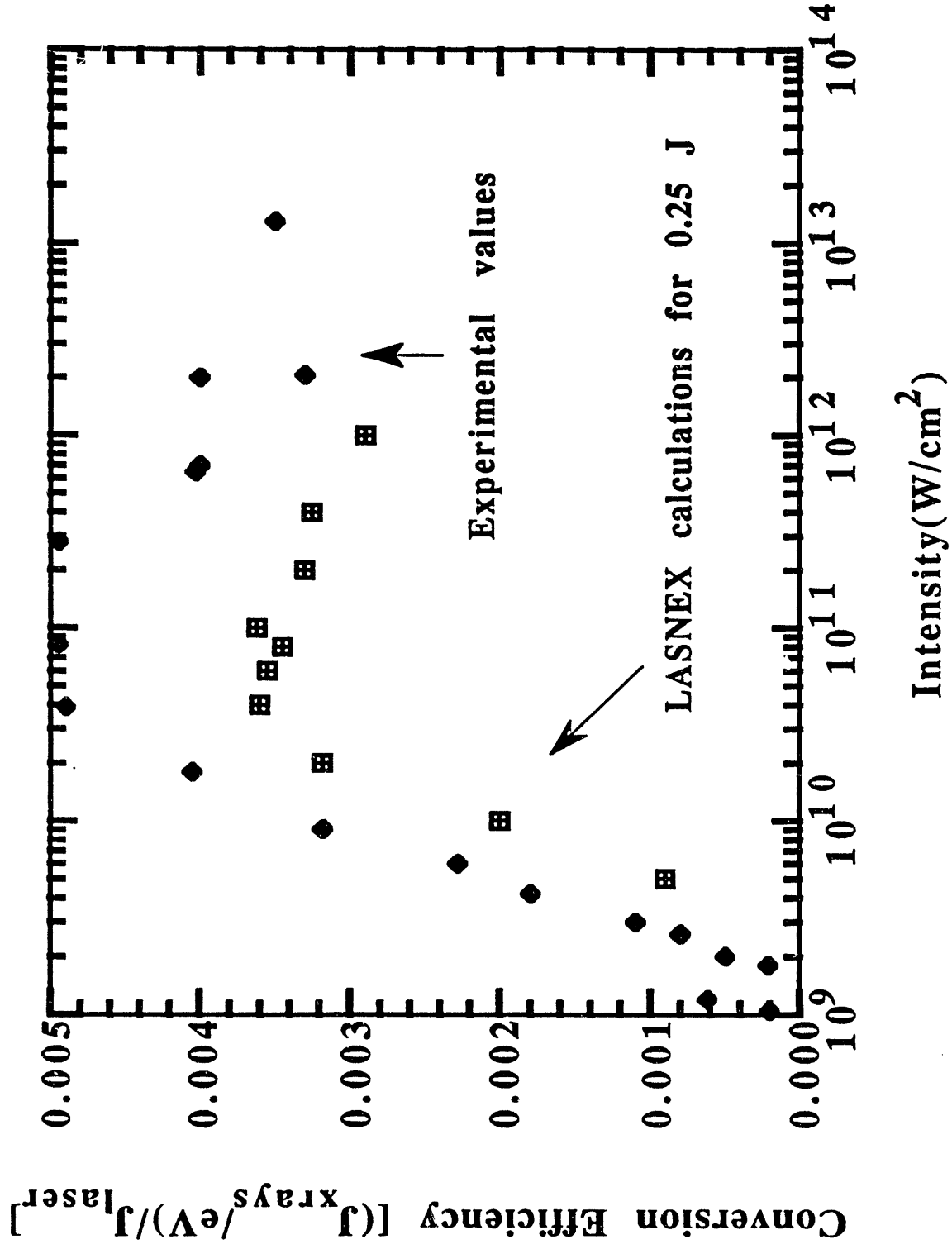


Figure 1

END

**DATE
FILMED**

10 / 6 / 93

